



## Effects of heat generation/absorption on natural convection of nanofluids over the vertical plate embedded in a porous medium using drift-flux model

M. Ghalambaz and A. Noghrehabadi\*

*Department of Mechanical Engineering, Shahid Chamran University of Ahvaz, Ahvaz, Iran*

---

### Article info:

Received: 29/04/2012  
Accepted: 10/09/2013  
Online: 03/03/2014

---

### Keywords:

Nanofluid,  
Natural convection,  
Porous media,  
Heat generation,  
Drift flux model.

### Abstract

In this paper, natural convection heat transfer over a vertical plate in a Darcy porous medium saturated with a nanofluid subject to heat generation/absorption was theoretically studied. The governing partial differential equations were transformed to a set of ordinary differential equations using similarity transformations and solved using finite difference method. The influence of parametric variation of the Brownian motion parameter, thermophoresis parameter and heat generation/absorption parameter on velocity, temperature and nanoparticles concentration profiles was graphically shown. Impact of non-dimensional parameters on the reduced Nusselt number and reduced Sherwood number was also investigated. The results showed that an increase in the heat generation/absorption parameter would increase temperature and velocity profiles; but, it would decrease concentration profiles. Increase of thermophoresis parameter increased magnitude of concentration profiles while not showing any significant effect on velocity and temperature profiles. The results also indicated that increase of Brownian motion parameter did not demonstrate any significant effect on the magnitude of velocity and temperature profiles. It was found that an increase in the heat generation/absorption parameter decreased the reduced Nusselt number whereas it increased the reduced Sherwood number. For negative values of the Brownian motion parameter, increase of the thermophoresis parameter increased the reduced Nusselt and Sherwood numbers.

---

### Nomenclature

$(x, y)$	Cartesian coordinates	$g$	Gravitational acceleration vector
$D_B$	Brownian diffusion coefficient	$K$	Permeability of the porous medium
$D_T$	Thermophoretic diffusion coefficient	$k$	Thermal conductivity
$f$	Rescaled nano particle volume fraction, nano particle concentration	$k_m$	Effective thermal conductivity of the

---

\* Corresponding author:

Email address: [noghrehabadi@scu.ac.ir](mailto:noghrehabadi@scu.ac.ir)

	porous medium
$Le$	Lewis number
$m$	Number of grid points
$Nb$	Brownian motion parameter
$Nr$	Buoyancy ratio
$Nt$	Thermophoresis parameter
$P$	Pressure
$Q_0$	Heat generation coefficient
$Ra_x$	Local Rayleigh number
$S$	Dimensionless stream function
$T$	Temperature
$T_\infty$	Ambient temperature
$T_w$	Wall temperature of the vertical plate
$U$	Reference velocity
$u, v$	Darcy velocity components

**Greek symbols**

$(\rho c)_f$	Heat capacity of the nanofluid
$(\rho c)_m$	Effective heat capacity of porous medium
$(\rho c)_p$	Effective heat capacity of nano particles material
$\mu$	Viscosity of nanofluid
$\alpha_m$	Thermal diffusivity of the porous medium
$\beta$	Volumetric expansion coefficient of fluid
$\varepsilon$	Porosity
$\eta$	Dimensionless distance
$\theta$	Dimensionless temperature
$\lambda$	Heat generation or absorption parameter defined by Eq. (16e)
$\rho_f$	Fluid density
$\rho_p$	Nano particle density
$\tau$	Parameter defined by Eq. (7)
$\varphi$	Nano particle volume fraction
$\varphi_\infty$	Ambient nano particle volume fraction
$\varphi_w$	Nano particle volume fraction at the surface
$\psi$	Stream function

**1. Introduction**

Studying boundary layer flow and heat transfer over a vertical or horizontal flat plate has gained great attention [1-8]. Analysis of natural convection heat transfer over the flat plate embedded in a porous medium is very important because of its many engineering applications such as thermal energy storage, groundwater systems, flow through filtering media and crude oil extraction [4]. Among these applications, convection in a porous

medium with internal energy sources is practical in the theory of thermal ignition and in problems dealing with chemical reactions and those concerned with dissociating fluids [3,5]. The problem of free convection from a vertical plate with non-uniform surface temperature has been previously studied by Gorla and Zinalabedini (1987) [7]. Likewise, similarity solution of natural convection boundary layer flow along the vertical plate subject to variable wall temperature has been investigated by Cheng and Minkowycz [8].

Although natural convection flow and heat transfer over embedded bodies in porous medium has been studied in a large number of papers, few works have considered flow and heat transfer of nanofluids. Nanofluids are suspensions of submicronic particles (nanoparticles) in a conventional fluid. The most important characteristic of nanofluids is their high thermal conductivity relative to base fluids, which can be achieved even at very low volume fraction of nanoparticles. In recent years, heat transfer enhancement of nanofluids has been proposed as a route for surpassing performance of heat transfer rate in the currently available liquids [9-11]. The fluid containing nanoparticles can smoothly flow through microchannels without clogging them because nanoparticles are small enough to behave similar to liquid molecules [9,10]. The unique property of nanofluids in enhancing heat transfer has attracted the attention of many researchers. Convective heat transfer of nanofluids has been analyzed in many previous studies [4-6, 12-15]. Most researchers have reported that the presence of nanoparticles in the base fluid enhances its effective thermal conductivity and consequently enhances heat transfer characteristics [16]. An excellent review of thermo-physical properties of nanofluids can be found in the review by Khanafer and Vafai [17].

Buongiorno [18] discussed seven possible mechanisms for fluid particle slip during convection of nanofluids, out of which only thermophoresis and the Brownian diffusion were found to be important [18].

Using the non-homogeneous models, mixed convective boundary layer flow over the vertical wedge embedded in a porous medium saturated with a nanofluid subject to natural convection dominated regime was analyzed by Gorla et al. [4]. The non-Darcy natural convection of nanofluids over the isothermal cone embedded in a porous medium was analyzed by Noghrehabadi et al. [19]. Natural convective boundary layer flow over the horizontal plate embedded in a nanofluid-saturated porous medium was also investigated by Gorla and Chamkha [20]. Noghrehabadi et al. [21] analyzed the Darcy flow and natural convection heat transfer of nanofluids over a vertical flat plate prescribed heat flux boundary condition. The Cheng–Minkowycz problem for natural convective boundary-layer flow in a porous medium which was saturated by a nanofluid was examined by Nield and Kuznetsov [22].

In the present study, effect of heat generation/absorption on the boundary layer heat and mass transfer of nanofluids over an isothermal flat plate was theoretically examined. A drift-flux, four equation models was utilized to consider slip velocity of nanoparticles in the base fluid because of Brownian motion and thermophoresis effects.

**2. Governing equations**

Consider a two-dimensional problem and steady natural convection boundary layer flow past along a vertical plate placed in a porous medium saturated with nanofluid in the presence of heat generation/absorption. Coordinate system is chosen such that x-axis is aligned with the flow over the plate. The scheme of physical model and coordinate system is illustrated in Fig. 1.

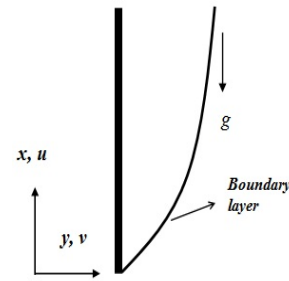


**Fig. 1.** Physical model and coordinate system.

Although there are three distinct boundary layers namely, hydrodynamic boundary layer (velocity), thermal boundary layer (temperature) and nanoparticle concentration boundary layer (concentration) over the plate, only one boundary layer is depicted in this figure to avoid congestion. It is assumed that the plate temperature is constant, and its higher than the temperature of ambient. The nanoparticles volume fraction ( $\phi$ ) at the wall surface ( $y=0$ ) takes the constant value of  $\phi_w$ . In the boundary layer, the heat is either generated or absorbed with the rate of  $Q_0$  where  $Q_0$  is negative in the case of heat absorption and positive in case of heat generation. The ambient values of  $T$  and  $\phi$  are denoted by  $T_\infty$  and  $\phi_\infty$ , respectively. The flow in the porous medium with porosity of  $\epsilon$  and permeability of  $K$  is considered as Darcy flow. It is also assumed that the nanofluid and porous medium are homogeneous and in local thermal equilibrium. By employing the Oberbeck-Boussinesq approximation and applying the standard boundary layer approximations, the basic steady conservation of total mass, momentum, thermal energy, and nanoparticles for nanofluids in the Cartesian coordinate system of  $x$  and  $y$  as follows [21, 22]:

$$\frac{\partial u}{\partial x} + \frac{\partial v}{\partial y} = 0, \tag{1}$$

$$\frac{\partial p}{\partial y} = 0, \tag{2a}$$

$$\frac{\mu}{K}u = \left[ -\left(\frac{\partial p}{\partial x} - (1-\phi_\infty)\beta g \rho_{f_\infty} (T - T_\infty)\right) \right. \\ \left. - (\rho_p - \rho_{f_\infty})g(\phi - \phi_\infty) \right] \tag{2b}$$

$$u \frac{\partial T}{\partial x} + v \frac{\partial T}{\partial y} = \alpha_m \frac{\partial^2 T}{\partial y^2} + \tau \left[ D_B \frac{\partial \phi}{\partial y} \frac{\partial T}{\partial y} + \frac{D_T}{T_\infty} \left(\frac{\partial T}{\partial y}\right)^2 \right] \\ + \frac{Q_0}{\rho c_p} (T - T_\infty), \tag{3}$$

$$\frac{1}{\varepsilon} \left[ u \frac{\partial \phi}{\partial x} + v \frac{\partial \phi}{\partial y} \right] = D_B \frac{\partial^2 \phi}{\partial y^2} + \left(\frac{D_T}{T_\infty}\right) \frac{\partial^2 T}{\partial y^2}, \tag{4}$$

and subject to the following boundary conditions,

$$v = 0, T = T_w, \phi = \phi_w, \text{ at } y = 0 \tag{5a}$$

$$u \rightarrow u_\infty, T \rightarrow T_\infty, \phi \rightarrow \phi_\infty, \text{ at } y \rightarrow \infty \tag{5b}$$

where

$$\alpha_m = \frac{k_m}{(\rho c)_f}, \quad \tau = \frac{\varepsilon(\rho c)_p}{(\rho c)_f}, \tag{6}$$

In Eq. (3), heat generation model is based on the previous studies [3, 5, and 6]. Pressure,  $P$ , can be eliminated from the momentum equations, *i.e.* Eqs. (2a) and (2b), by cross-differentiation. By introducing the following stream function ( $\psi$ ), the continuity equation is satisfied:

$$u = \frac{\partial \psi}{\partial y}, \quad v = -\frac{\partial \psi}{\partial x}, \tag{7}$$

Here is the local Rayleigh number,  $Ra_x$ , introduced as:

$$Ra_x = \frac{(1-\phi_\infty)\rho_{f_\infty}\beta Kgx(T_w - T_\infty)}{\mu\alpha_m}, \tag{8}$$

where  $\eta$  is similarity variable,

$$\eta = \frac{y}{x} Ra_x^{\frac{1}{2}}, \tag{9}$$

and dimensionless similarity quantities  $S$ ,  $\theta$ , and  $f$  are defined by,

$$S = \frac{\psi}{\alpha_m Ra_x^{\frac{1}{2}}}, \quad f = \frac{\phi - \phi_\infty}{\phi_w - \phi_\infty}, \quad \theta = \frac{T - T_\infty}{T_w - T_\infty}, \tag{10}$$

By applying Eqs. (9) and (10) to Eqs. (1-4), the following three ordinary differential equations are obtained,

$$S'' - \theta' + Nr.f' = 0, \tag{11}$$

$$\theta'' + \frac{1}{2}S\theta' + Nb.f'\theta' + Nt(\theta')^2 + \lambda.\theta = 0, \tag{12}$$

$$f'' + \frac{1}{2}Le.S.f' + \frac{Nt}{Nb}\theta'' = 0, \tag{13}$$

which are subject to the following boundary conditions:

$$\eta = 0: \quad S=0, \quad \theta=1, \quad f=1 \tag{14a}$$

$$\eta \rightarrow \infty: \quad S'=0, \quad \theta=0, \quad f=0 \tag{14b}$$

where

$$Nr = \frac{(\rho_p - \rho_{f_\infty})(\phi_w - \phi_\infty)}{\rho_{f_\infty}\beta(T_w - T_\infty)(1-\phi_\infty)}, \tag{15a}$$

$$Nb = \frac{\varepsilon(\rho c)_p D_B (\phi_w - \phi_\infty)}{(\rho c)_f \alpha_m}, \tag{15b}$$

$$Nt = \frac{\varepsilon(\rho c)_p D_T (T_w - T_\infty)}{(\rho c)_f \alpha_m T_\infty}, \tag{15c}$$

$$Le = \frac{\alpha_m}{\varepsilon D_B}, \tag{15d}$$

$$\lambda = \frac{\mu Q_0 x}{(1-\phi_\infty)\rho_{f_\infty}^2 c_p \beta g (T_w - T_\infty)}, \tag{15e}$$

In the above equations, in which  $Q_0$  varies with inverses of position ( $1/x$ ), the obtained equations are in the form of fully similarity solution; otherwise, they are in the form of local similarity. In the following text, the case of fully similarity solution is considered. Here,  $Nr$  is bouncy ratio parameter,  $Nb$  is Brownian motion parameter,  $Nt$

is thermophoresis parameter,  $Le$  is Lewis number and  $\lambda$  is heat generation/absorption parameter.

Quantities of local Nusselt number ( $Nu_x$ ) and local Sherwood number ( $Sh_x$ ) can be introduced by [16]:

$$Nu_x = \frac{q_w x}{k (T_w - T_\infty)}, \tag{16}$$

$$Sh_x = \frac{q_m x}{D_B (\phi_w - \phi_\infty)}, \tag{17}$$

where quantity of  $q_w$  indicates the wall heat flux because of temperature gradient and  $q_m$  indicates mass flux because of the effect of Brownian motion. Using similarity transforms in Eq. (10), reduced Nusselt number ( $Nur$ ) and reduced Sherwood number ( $Shr$ ) as important parameters in heat and mass transfer are obtained as:

$$Ra_x^{-\frac{1}{2}} Nu_x = -\theta'(0) \tag{18a}$$

$$Ra_x^{-\frac{1}{2}} Sh_x = -f'(0) \tag{18b}$$

### 3. Numerical method

Eqs. (11-13) represent a boundary value problem and these general non-linear equations cannot be solved in a closed form. In this case, a numerical solution method is necessary to describe physics of the problem. Finite difference methods as well as finite element methods are the techniques, which have been widely employed to solving ordinary as well as partial differential equations governing the boundary value problems [23 and 24]. The explicit, iterative, finite difference method is simple and adequate for solving boundary value problems [25]. Therefore, in this study, explicit, iterative, finite difference method was adopted to solve the present differential equations. Following the finite difference method, all of the first-order and second-order derivative terms with respect to  $\eta$  in system of Eqs. (12-14) were discretized using three-point central difference formula, written as:

$$\frac{S_{i+1} - 2S_i + S_{i-1}}{\Delta\eta^2} - \frac{\theta_{i+1} - \theta_{i-1}}{2\Delta\eta} + Nr \cdot \frac{f_{i+1} - f_{i-1}}{2\Delta\eta} = 0 \tag{19}$$

$$\frac{\theta_{i+1} - 2\theta_i + \theta_{i-1}}{\Delta\eta^2} + \frac{1}{2} S_i \cdot \left( \frac{\theta_{i+1} - \theta_{i-1}}{2\Delta\eta} \right) + Nb \cdot \left( \frac{f_{i+1} - f_{i-1}}{2\Delta\eta} \right) \cdot \left( \frac{\theta_{i+1} - \theta_{i-1}}{2\Delta\eta} \right) + Nt \cdot \left( \frac{\theta_{i+1} - \theta_{i-1}}{2\Delta\eta} \right)^2 + \lambda \theta_i = 0 \tag{20}$$

$$\frac{f_{i+1} - 2f_i + f_{i-1}}{\Delta\eta^2} + \frac{1}{2} Le S_i \cdot \left( \frac{f_{i+1} - f_{i-1}}{2\Delta\eta} \right) + \frac{Nt}{Nb} \cdot \left( \frac{\theta_{i+1} - 2\theta_i + \theta_{i-1}}{\Delta\eta^2} \right) = 0 \tag{21}$$

where  $\Delta\eta$  is step length in the  $\eta$  direction. Since the above equations are non-linear and coupled, they cannot be exactly solved. Therefore, an iterative scheme is required to be used. In order to perform an iterating procedure, Eqs. (19-21) are written in the following form:

$$S_i = \frac{S_{i+1} + S_{i-1}}{2} - \Delta\eta \left( \frac{\theta_{i+1} - \theta_{i-1}}{4} \right) + Nr \cdot \Delta\eta \cdot \left( \frac{f_{i+1} - f_{i-1}}{4} \right) \tag{22}$$

$$\theta_i = \frac{\theta_{i+1} + \theta_{i-1}}{2 - \Delta\eta^2 \cdot \lambda} + \frac{1}{2} S_i \cdot \left( \frac{\theta_{i+1} - \theta_{i-1}}{\Delta\eta} \right) + Nb \cdot \left( \frac{f_{i+1} - f_{i-1}}{\Delta\eta} \right) \cdot \left( \frac{\theta_{i+1} - \theta_{i-1}}{\Delta\eta} \right) + Nt \cdot \left( \frac{\theta_{i+1} - \theta_{i-1}}{\Delta\eta} \right)^2 \tag{23}$$

$$f_i = \frac{f_{i+1} + f_{i-1}}{2} + \frac{1}{2} Le S_i \cdot \Delta\eta \cdot \left( \frac{f_{i+1} - f_{i-1}}{4} \right) + \frac{Nt}{Nb} \cdot \left( \frac{\theta_{i+1} - 2\theta_i + \theta_{i-1}}{2} \right) \tag{24}$$

and boundary conditions are as follows:

$$S_1 = 0, \quad \theta_1 = 1, \quad f_1 = 1 \tag{25a}$$

$$S_{m+2} - S_m = 0, \quad \theta_{m+1} = 0, \quad f_{m+1} = 0 \tag{25b}$$

where  $m$  is number of grid points. Considering the system of Eqs. (22-24) subject to boundary conditions (25a-b) and commencing with an initial guess values, new iterative values can be easily obtained. This process continues until the absolute error ( $x_i - x_{i-1}$ ) in the entire domain of the solution is less than the required accuracy. Critical point of this method is selection of appropriate asymptotic value of  $\eta_\infty$ . In the present study,  $\eta_\infty$  is taken to be 10, which ensures asymptotic convergence of the solution. Then,  $\eta$  direction is divided to  $m=10000$  nodal points so that the results become accurate. A maximum relative error of  $10^{-5}$  is used as the stopping criteria for the iterations.

As a test of the solution accuracy, value of  $Nur$  is compared with the value reported by Cheng and Minkowycz [8] in Table 1 and effects of nanofluid parameters and heat generation/absorption parameter were neglected in this study.

**Table 1.** Comparing the present results and those of Cheng and Minkowycz  $-\theta'(0)$  in the case of pure fluid.

Cheng and Minkowycz [8]	Present result
0.4440	0.4439

Neglecting the Brownian motion and thermophoresis effects and in the absence of nanoparticles, the present work was reduced to natural convection of a pure fluid over the vertical plate embedded in a saturated porous medium, which was experimentally examined by Evans and Plumb [26]. They experimentally analyzed natural convection heat transfer about the isothermal vertical plate embedded in a porous medium composed of glass beads with diameters ranging from 0.85 to 1.68 mm. Here, results of the present study in the case of  $Nr=Nb=Nt=\lambda=0$  were compared with those reported by Evans and Plumb [26] in Fig. 2.

As seen, Fig. 2 shows very good agreement between the experimental results and the solution of Eqs. (11 and 12).

#### 4. Results and discussion

In the present study, values of heat generation parameter ( $\lambda$ ) were chosen to be in the range of  $-0.6 < \lambda < 0.15$  to clearly show effect of this parameter on dimensionless velocity, temperature and concentration profiles as well as reduced Nusselt number and reduced Sherwood number.

A similar, but narrower, range of heat generation parameter,  $-0.3 < \lambda < 0.1$ , was adopted by Hady *et al.* [5] to investigate effect of heat generation or absorption on natural convection heat transfer over the vertical full cone embedded in a porous medium saturated with a nanofluid. The chosen range for heat generation parameter allowed for a reasonable correspondence between the present work and the study of Hady *et al.* [5]. Most of the known nanofluids reported in the literatures have large values of Lewis number  $Le > 1$  [22].

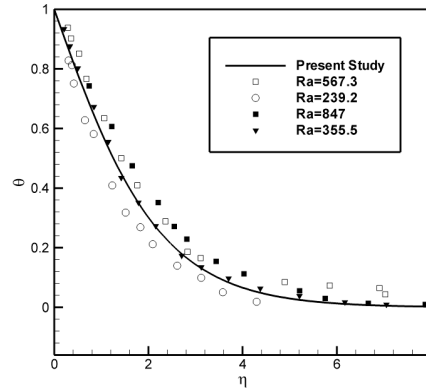


**Fig. 2.** Comparing the present study ( $Nr=Nb=Nt=\lambda=0$ ) and the experimental results reported by Evans and Plumb [26].

Both of the Brownian motion and thermophoresis parameters are small [18]. The thermophoresis parameter is positive [18] when temperature of the plate is higher than the ambient temperature; but, the Brownian motion parameter can adopt positive or negative values. Negative value of the Brownian motion parameter indicates that concentration of nanoparticles on the wall surface

is less than concentration of nanoparticles outside the boundary layer. Non-dimensional profiles of velocity, temperature and nanoparticles volume fraction are shown in Figs. (3-5), respectively, for different values of heat generation parameter ( $\lambda$ ) and selected values of thermophoresis parameter ( $Nt$ ). These figures indicate that an increase of heat generation parameter increases the magnitude of velocity and temperature profiles whereas decreasing the concentration profiles.

It is clear that heat generation in the boundary layer tended to increase temperature distribution; consequently, momentum of nanofluid was increased by increasing temperature profiles; thereby, velocity profiles increased. By contrast, increasing heat generation/absorption exacerbated the nanoparticles deposition away from the surface into the fluid and thus concentration profiles were decreased. The thermophoresis parameter ( $Nt$ ) could be described as ratio of the nanoparticles diffusion, which was due to the thermophoresis effect, to the thermal diffusion in the nanofluid.

Thermophoresis applied a force to nanoparticles opposite to the temperature gradient, which was proportional to the temperature gradient. Hence, increase of temperature gradient increased the thermophoresis force and thereby diffusion of nanoparticles. Fig. 6 shows variation of non-dimensional profiles for different values of thermophoresis parameter ( $Nt$ ) when the buoyancy-ratio parameter, Brownian motion parameter and Lewis number were constant and the heat generation/absorption parameter was taken to be zero.

By increasing  $Nt$ , thermophoresis force increased, which tended to move particles from hot to cold. Therefore, increase of  $Nt$  increased the nanoparticle concentration, as shown in Fig. 6. In addition, increase in the thermophoresis parameter did not show any significant effect on the dimensionless temperature and velocity profiles.

The Brownian motion parameter can be described as ratio of nanoparticles diffusion,

which is due to the Brownian motion effect, to the thermal diffusion in the nanofluid.

Fig. 7 shows variation of non-dimensional velocity, temperature and nanoparticles concentration profiles for different values of Brownian motion parameter ( $Nb$ ) when the buoyancy-ratio parameter, thermophoresis parameter and Lewis number were constant and the heat generation/absorption parameter was taken to be zero.

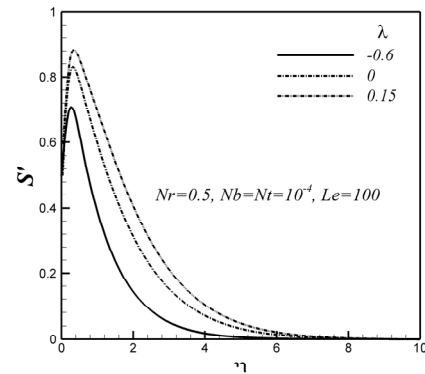


Fig. 3. Velocity profiles for various values of heat generation/absorption parameter.

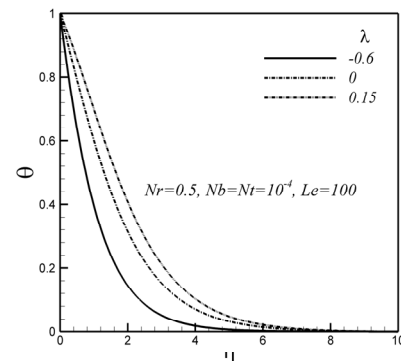


Fig. 4. Temperature profiles for various values of heat generation/absorption parameter.

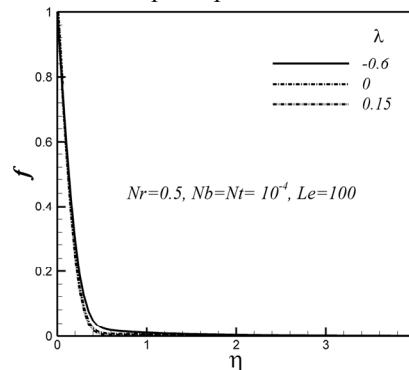
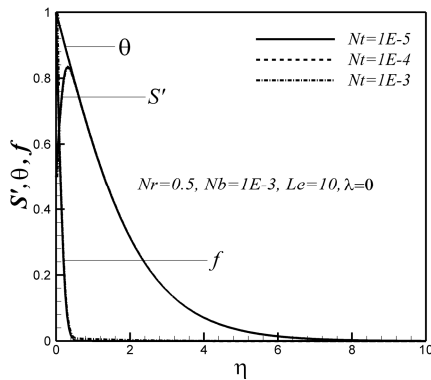


Fig. 5. Volume fraction profiles for various values of heat generation/absorption parameter.



**Fig. 6.** Velocity, temperature and nanoparticles concentration profiles for various values of the thermophoresis parameter.

Fig. 7 depicts that increase of the Brownian motion parameter did not show any significant influence on the temperature profiles whereas increasing velocity profiles and decreasing the nanoparticles concentration profiles. In addition, a raise in the Brownian motion parameter exacerbated particle deposition away from the surface into the fluid when  $Nb > 0$ . Finally, the values of heat generation/absorption parameter ( $\lambda$ ) in the range of  $\lambda = 0.1$  to  $\lambda = -0.1$  were chosen to denote effect of heat generation/absorption parameter on the reduced Nusselt number and reduced Sherwood number. Figures 8 and 9 reveal that an increment in the heat generation/absorption parameter would decrease magnitude of reduced Nusselt number whereas it would increase magnitude of reduced Sherwood number. As observed in Fig. 4, augmentation of heat generation parameter declined the magnitude of temperature gradient on the wall surface and thereby led to decrease of the reduced Nusselt number. As observed in Fig. 5, magnitude of concentration gradient on the wall increased with a raise in the heat generation/absorption parameter. Augmentation of the heat generation parameter decreased the concentration boundary layer thickness, which consequently resulted in the increase of reduced Sherwood number. Furthermore, in the case of positive value of the Brownian motion parameter ( $Nb = 1.0 \times 10^{-4}$ ), increase of the thermophoresis parameter

slightly decreased the reduced Nusselt number. However, augmentation of thermophoresis parameter obviously decreased the reduced Sherwood number. Hady et al. [5] reported that, as heat generation/absorption parameter ( $\lambda$ ) increased, the local Nusselt number decreased, which was in good agreement with results of the present study.

Figures 10 and 11 show effect of negative and positive values of Brownian motion parameter on the reduced Nusselt number and reduced Sherwood number, respectively. These figures indicate that, for the positive values of Brownian motion parameter, an increase of the Brownian motion parameter increased the reduced Nusselt number and reduced Sherwood number.

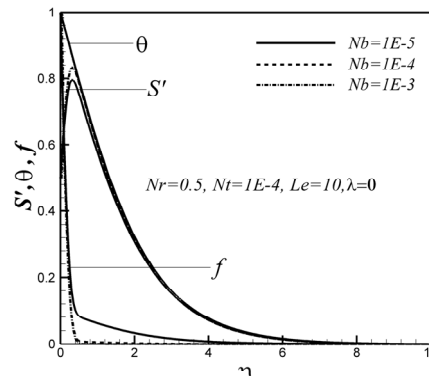


**Fig. 7.** Velocity, temperature and nanoparticles concentration profiles for various values of the Brownian motion parameter.

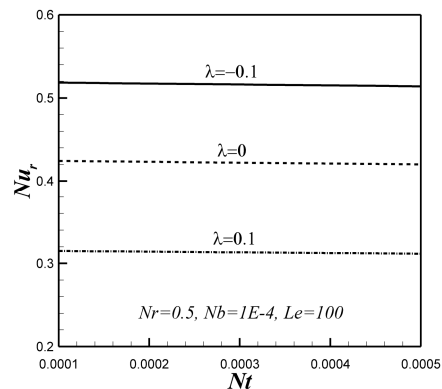


**Fig. 8.** Reduced Nusselt number profiles for various values of heat generation/absorption and thermophoresis parameter.

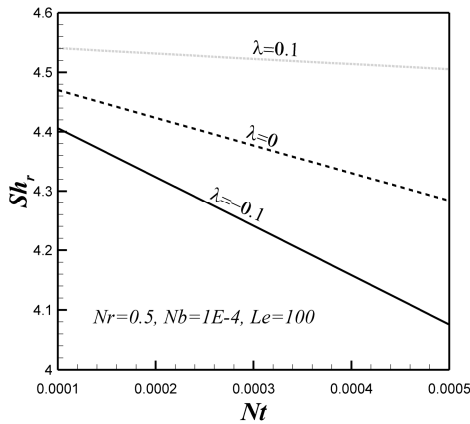


**Fig. 9.** Reduced Sherwood number profiles for various values of heat generation/absorption and thermophoresis parameter.

Likewise, in the case of negative values of Brownian motion parameter, an increase of the magnitude of the Brownian motion parameter increased the reduced Nusselt number and Sherwood numbers.

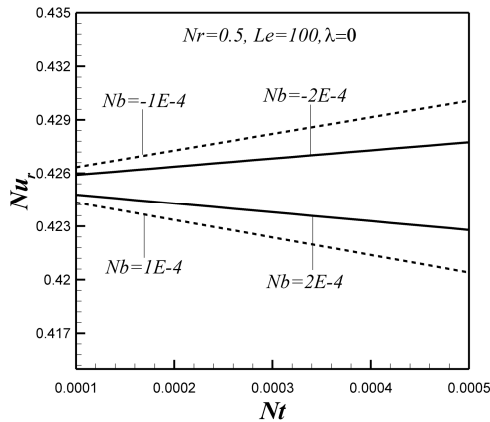


**Fig. 10.** Reduced Nusselt number profiles for various values of  $Nb$  and  $Nt$ .

It is worth noticing that variation of the reduced Nusselt number was very slight as a result of varying thermophoresis parameter.

### 5. Conclusions

A combined similarity and numerical approach was utilized to theoretically investigate natural convection from the vertical plate embedded in a nanofluid-saturated porous medium with heat generation/absorption. In modeling the nanofluid, thermophoresis and Brownian

motion effects were taken into account. The results can be summarized as follows:

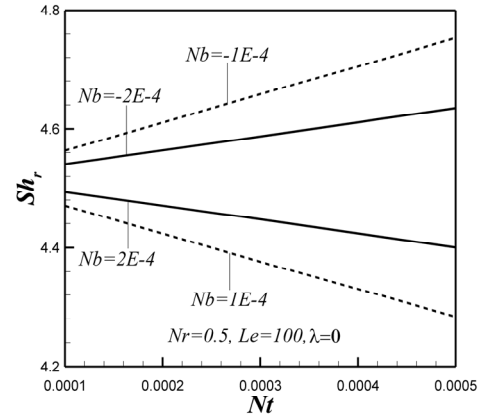


**Fig. 11.** Reduced Sherwood number profiles for various values of  $Nb$  and  $Nt$ .

- 1) Increase of heat generation/absorption parameter increased velocity and temperature profiles; but, it decreased nanoparticles concentration profiles in the boundary layer.
- 2) An increase in the heat generation/absorption parameter would decrease the reduced Nusselt number but increase reduced Sherwood number.
- 3) Increase of thermophoresis parameter increased magnitude of concentration profiles while not showing any significant effect on velocity and temperature profiles.
- 4) Increase of Brownian motion parameter did not show any significant influence on magnitude of velocity and temperature profiles; but, its effect on concentration profiles was considerable in the vicinity of the wall. Increase of the Brownian motion parameter decreased thickness of the concentration boundary layer.
- 5) For negative values of Brownian motion parameter, increase of thermophoresis parameter increased the reduced Nusselt and Sherwood numbers. In contrast, in the case of positive values of Brownian motion parameter, the reduced Nusselt and Sherwood numbers were increasing functions of the thermophoresis parameter. Effect of variation of thermophoresis parameter on the reduced Nusselt Number was very slight.

### Acknowledgements

The authors are grateful to Shahid Chamran University of Ahvaz for its support. They also would like to thank Ali Behseresht for his considerable effort in analyzing the results of this paper.

### References

- [1] T. Sudhakar Reddy, M. C. Rajub and S. V. K. Varmc, "Chemical reaction and radiation effects on MHD free convection flow through a porous medium bounded by a vertical surface with constant heat and mass flux", *Journal of Computational and Applied Research in Mechanical Engineering*, Vol. 3, No. 1, pp. 53-62, (2013).
- [2] A. Noghrehabadi, M. Ghalambaz and A. Samimi, "Approximate solution of laminar thermal boundary layer over a thin plate heated from below by convection", *Journal of Computational and Applied Research in Mechanical Engineering*, Vol. 2, No. 2, pp. 45-57, (2013).
- [3] M. Gnaneswara Reddy, "Heat generation and radiation effects on steady MHD free convection flow of micropolar fluid past a moving surface", *Journal of Computational and Applied Research in Mechanical Engineering*, Vol. 2, No. 2, pp. 1-10 (2013).
- [4] R. S. R. Gorla, A. J. Chamkha and A. M. Rashad, "Mixed convective boundary layer flow over a vertical wedge embedded in a porous medium saturated with a nanofluid- Natural Convection Dominated Regime", *Nanoscale Res. Lett.*, Vol. 6, No. 1, pp. 1-9, (2011).
- [5] F. M. Hady, F. S. Ibrahim, S. M. Abdel-Gaied and M. R. Eid "Effect of heat generation/absorption on natural convective boundary-layer flow from a vertical cone embedded in a porous medium filled with a non-Newtonian nanofluid", *Int. Commun. Heat Mass*. Vol. 38, No. 10, pp. 1414-1420, (2011).
- [6] A. Noghrehabadi, M. R. Saffarian, R. Pourrajab and M. Ghalambaz, "Entropy analysis for nanofluid flow over a stretching sheet in the presence of heat generation/absorption and partial slip", *J. Mech. Sci. Technol.*, Vol. 27, No. 3, pp. 927-937, (2013).
- [7] R. S. R. Gorla and A. Zinolabedini "Free convection from a vertical plate with nonuniform surface temperature and embedded in a porous medium", *J. Energ. Resour.-ASME*, Vol. 109, No. 1, pp. 26-30, (1987).
- [8] P. Cheng and W. J. Minkowycz, "Free convection about a vertical flat plate embedded in a saturated porous medium with applications to heat transfer from a dike", *J. Geophysics. Res.*, Vol. 82, No. 14, pp. 2040-2044, (1977).
- [9] W. Yu, D. M. France and J. L. Routbort, "Review and comparison of nanofluid thermal conductivity and heat transfer enhancements", *Heat Transfer Eng.*, Vol. 29, No. 5, pp. 432-460, (2008).
- [10] W. Daungthongsuk and S. Wongwises, "A critical review of convective heat transfer of nanofluids", *Renew. Sust. Energ. Rev.*, Vol. 11, No. 5, pp. 797-817, (2007).
- [11] K. S. Hwang, S. P. Jang and S. U. Choi, "Flow and convective heat transfer characteristics of water-based Al<sub>2</sub>O<sub>3</sub> nanofluids in fully developed laminar flow regime", *Int. J. Heat Mass Tran.*, Vol. 52, No. 1, pp. 193-199, (2009).
- [12] A. Noghrehabadi, R. Pourrajab and M. Ghalambaz, "Flow and heat transfer of nanofluids over stretching sheet taking into account partial slip and thermal convective boundary conditions", *Heat Mass Transfer*, Vol. 49, pp. 1357-1366, (2013).
- [13] A. Noghrehabadi, R. Pourrajab and M. Ghalambaz, "Effect of partial slip boundary condition on the flow and heat transfer of nanofluids past stretching sheet prescribed constant wall temperature", *Int.*

- J. Therm. Sci.*, Vol. 54, pp. 253-261, (2012).
- [14] A. Noghrehabadi, M. Ghalambaz, M., Ghalambaz and A. Ghanbarzadeh, "Comparing thermal enhancement of Ag-water and SiO<sub>2</sub>-water nanofluids over an isothermal stretching sheet with suction or injection", *Journal of Computational and Applied Research in Mechanical Engineering*, Vol. 2, No. 1, pp. 35-47, (2012).
- [15] A. Noghrehabadi, M. Ghalambaz and A. Ghanbarzadeh, "Heat transfer of magnetohydrodynamic viscous nanofluids over an isothermal stretching sheet", *J. Thermophys. Heat Tr.*, Vol. 26, No. 4, pp. 686-689, (2012).
- [16] S. K. Das, S. U. S. Choi, W. Yu and T. Pradeep, *Nanofluids: Science and Technology*, John Wiley & Sons, New Jersey, Canada, (2007).
- [17] K. Khanafer and K. Vafai, "A critical synthesis of thermophysical characteristics of nanofluids", *Int. J. Heat Mass Tran.*, Vol. 54, No. 19, pp. 4410-4428, (2011).
- [18] J. Buongiorno, "Convective transport in nanofluids", *J. Heat Trans.-T. ASME*, Vol. 128, No. 3, pp. 240-250, (2006).
- [19] A. Noghrehabadi, A. Behseresht, M. Ghalambaz and J. Behseresht, "Natural-convection flow of nanofluids over vertical cone embedded in non-darcy porous media", *J. Thermophys. Heat Tr.*, Vol. 27, No. 2, pp. 334-341, (2013).
- [20] R. S. R. Gorla and A. Chamkha, "Natural convective boundary layer flow over a horizontal plate embedded in a porous medium saturated with a nanofluid", *Journal of Modern Physics*, Vol. 2, No. 2, pp. 62-71, (2011).
- [21] A. Noghrehabadi, A. Behseresht and M. Ghalambaz, "Natural convection of nanofluid over vertical plate embedded in porous medium: prescribed surface heat flux", *Appl. Math. Mech. -Engl. Ed.*, Vol. 34, No. 6, pp. 669-686, (2013).
- [22] D. A. Nield and A. V. Kuznetsov, "The Cheng-Minkowycz problem for natural convective boundary-layer flow in a porous medium saturated by a nanofluid", *Int. J. Heat Mass Tran.* Vol. 52, No. 25, pp. 5792-5795, (2009).
- [23] M. Hoseinpour Gollo, H. Moslemi Naeini and N. B. Mostafa Arab, "Experimental and numerical investigation on laser bending process", *Journal of Computational and Applied Research in Mechanical Engineering*, Vol. 1, No. 1, pp. 45-52, (2011).
- [24] B. Jamshidi, F. Haji Aboutalebi, M. Farzin, "Finite element prediction of ductile fracture in automotive panel forming: comparison between FLD and lemaître damage models", *Journal of Computational and Applied Research in Mechanical Engineering*, Vol. 1, No. 1, pp. 37-44, (2011).
- [25] J. F. Wendt and J. D. Anderson, *Computational Fluid Dynamics: an Introduction*, Springer, (2009).
- [26] G. H. Evans, and O. A. Plumb, "Natural convection from a vertical isothermal surface embedded in a saturated porous medium". *AIAA-ASME Thermophysics and Heat Transfer Conf.*, Palo Alto, California, Paper 78-HT -55. In: Nield, D., Bejan, A., *Convection in Porous Media*, Springer New York, pp. 166-167, (2013).